Articles

Kinetic and Structural Characterization of Spinach Carbonic Anhydrase†

Roger S. Rowlett,*,‡ Mark R. Chance,§ Michael D. Wirt,§ Dean E. Sidelinger,§ Jill R. Royal,‡ Melanie Woodroffe,‡ Ying-Fuh A. Wang,‡ Rajib P. Saha,‡ and Michael G. Lam‡

Department of Chemistry, Colgate University, 13 Oak Drive, Hamilton, New York 13346, and the Department of Physiology and Biophysics, Albert Einstein College of Medicine of Yeshiva University, Bronx, New York 10461

Received July 1, 1994; Revised Manuscript Received September 19, 1994®

ABSTRACT: We have carried out kinetics studies of spinach carbonic anhydrase (CA) using stopped-flow spectrophotometry at steady state and ^{13}C-NMR exchange at chemical equilibrium. We found that the rate of $CO_2 \rightleftharpoons HCO_3^-$ exchange catalyzed by spinach CA at pH 7.0 to be 3−5 times faster than the maximal k_{cat} for either CO_2 hydration or HCO_3^- dehydration at steady state, suggesting a rate-determining H^+ transfer step in the catalytic mechanism. Correspondingly, we measured a pH-independent solvent deuterium isotope effect on k_{cat} of approximately 2.0, and found that the rate of catalysis was significantly decreased at external buffer concentrations below 5 mM. Our results are consistent with a zinc-hydroxide mechanism of action with for spinach CA, similar to that of animal carbonic anhydrases. We have also collected X-ray absorption spectra of spinach CA. Analysis of the extended fine structure (EXAFS) suggests that the coordination sphere of Zn in spinach CA must have one or more sulfur ligands, in contrast to animal CAs which have only nitrogen and oxygen ligands. The models which best fit the data have average Zn−N(O) distances of 1.99−2.06 Å, average Zn−S distances of 2.31−2.32 Å, and a total coordination number of 4−6. We conclude that animal and spinach CAs are convergently evolved enzymes which are structurally quite different, but functionally equivalent.

Carbonic anhydrase (carbonate hydrolyase, EC 4.2.1.1) is a zinc-metalloenzyme that catalyzes the reaction

$$CO_2 + H_2O \rightleftharpoons HCO_3^- + H^+ \quad (1)$$

CA[1] is found in virtually every living organism, including vertebrates and invertebrates (Carter, 1972; Maren, 1967), plants (Reed & Graham, 1980), and bacteria (Brundell et al., 1972). The most well-known CAs are of mammalian origin, where there are now at least seven distinct types, designated CA I through VII (Tashian, 1989). CA I, II, and III have been fully structurally characterized by X-ray crystallography (Kannan et al., 1975; Liljas et al., 1972; Eriksson et al., 1988; Eriksson, 1988) and have been thoroughly characterized kinetically (Silverman & Lindskog, 1988; Silverman & Vincent, 1983).

All the extant structural and kinetic data point toward common structural themes and catalytic mechanisms for these well-studied CA isoenzymes. The typical mammalian CA contains a catalytically essential Zn^{2+} ion which is coordinated to three histidine residues. A fourth coordination site is occupied by an ionizable water molecule with a pK_a near 7.0 (Silverman & Lindskog, 1988). The maximum catalytic efficiency (k_{cat} for the CO_2 hydration reaction) of mammalian CAs ranges from 3×10^4 s^{-1} for CA III (Rowlett et al., 1991) to as high as 1×10^6 s^{-1} for CA II (Khalifah, 1971). Despite the wide range of catalytic efficiency of the mammalian CA isoenzymes, all are thought to follow a common mechanism of action, consisting of two temporally distinct chemical steps. A Zn^{2+}-bound hydroxide ion or water molecule is implicated in both steps. For CO_2 hydration, the first step in catalysis is the attack of a Zn^{2+}-bound hydroxide on CO_2 to yield a Zn^{2+}-bound HCO_3^- species. The HCO_3^- is subsequently replaced by water to yield a Zn^{2+}-bound water molecule (eqs 2 and 3). In a second, separate step, the original Zn^{2+}-bound hydroxide ion is regenerated by a hydrogen ion transfer step (eq 4).

$$\equiv Zn^{2+}-OH^- + CO_2 \rightleftharpoons \equiv Zn^{2+}-HCO_3^- \quad (2)$$

$$\equiv Zn^{2+}-HCO_3^- \rightleftharpoons \equiv Zn^{2+}-OH_2 + HCO_3^- \quad (3)$$

$$\equiv Zn^{2+}-OH_2 \rightleftharpoons \equiv Zn^{2+}-OH^- + H^+ \quad (4)$$

Equation 4, the H^+ transfer step, appears to be rate-limiting

†This work was supported by grants from the National Science Foundation (MCB-9205892 and CHE-9300589) and the Petroleum Research Fund, administered by the American Chemical Society (25211-B4). The operation and construction of beamline X9A at the National Synchroton Light Source was supported by a grant from the National Institutes of Health (RR01633). The National Synchroton Light Source is supported by the Division of Materials Sciences and the Division of Chemical Sciences of the Department of Energy.

* Author to whom correspondence should be addressed. E-mail: rrowlett@center.colgate.edu.

‡ Department of Chemistry, Colgate University.

§ Department of Physiology and Biophysics, Albert Einstein College of Medicine.

® Abstract published in *Advance ACS Abstracts,* November 1, 1994.

[1] Abbreviations: CA, carbonic anhydrase; SDS−PAGE, sodium dodecyl sulfate−polyacrylamide gel electrophoresis; MES, 2-(*N*-morpholino)ethanesulfonic acid; MOPS, 3-(*N*-morpholino)propanesulfonic acid; HEPES, 4-(2-hydroxyethyl)piperazineethanesulfonic acid; bicine, *N*,*N*-bis(2-hydroxyethyl)glycine; EXAFS, X-ray absorption fine structure spectroscopy; FT, Fourier transform.

0006-2960/94/0433-13967$04.50/0

for CAs I–III (Rowlett et al., 1991; Lindskog, 1984; Rowlett, 1984). To account for the highest k_{cat} values observed for mammalian CAs, the chemistry of H^+ transfer must be slightly more complicated than suggested by eq 4. In CA II, for example, it is buffer species in bulk solution, not water, that is the ultimate H^+ acceptor, and buffer concentrations above 10 mM are required for maximal enzyme activity (Jonssson et al., 1976; Rowlett & Silverman, 1982).

Plant CA was first isolated by Neish (1939) and is apparently an abundant enzyme in leaves, accounting for as much as 1% of all leaf proteins in parsley (Tobin, 1970). In higher plants, the enzyme appears to be concentrated principally in chloroplasts (Reed & Graham, 1980), although there are reports of cytoplasmic forms (Reed, 1979). There is some evidence that CA may be an important participant in carbon fixation during photosynthesis (Reed & Graham, 1971, 1977).

Compared to animal CAs, plant CAs are rather poorly understood, both structurally and mechanistically. Of the plant CAs, that from dicotyledenous plants is the most well-studied. In contrast to mammals, plants appear to possess high molecular weight, oligomeric forms of CA (Pocker & Ng, 1973; Tobin, 1970; Hatch & Burnell, 1990; Kandel et al., 1978; Johansson & Forsman, 1993; Aliev et al., 1986a,b). Recently, the amino acid sequences of CA from spinach (Fawcett et al., 1990; Burnell et al., 1990), pea (Roeske & Ogren, 1990), tobacco (Majeau & Coleman, 1992), and *Arabidopsis thaliana* (Raines et al., 1992) have been reported from the sequencing of c-DNA. While plant CA sequences are very similar to each other, they are totally inhomologous with animal CA sequences. Most striking is the low histidine content of plant CA, which suggests that amino acid residues other than histidine may serve a ligands to the catalytically essential Zn^{2+} ion in the plant enzyme.

The enzyme kinetics of dicotyledon CA have been examined for the spinach (Pocker & Ng, 1973, 1974; Pocker & Miksch, 1978), parsley (Tobin, 1970), and pea (Johansson & Forsman, 1993) forms, and at first glance appears to be similar to that of mammalian CA. The maximal k_{cat} for dicotyledon CA is in the range of 10^5–10^6 s^{-1} per subunit, and the maximal k_{cat}/K_m value is near 10^9 M^{-1} s^{-1}.

The structural and kinetics studies of plant CA to date either have not directly addressed or have left unresolved several important questions. What is the nature of the active site of plant CA? Specifically, what is the nature of the coordination sphere of the catalytically essential Zn^{2+} ion in plant CA? Is the kinetics of the plant CA-catalyzed reversible hydration of CO_2 consistent with a zinc-hydroxide mechanism, and if so, what is the rate-limiting step in catalysis? We describe here Zn-EXAFS and enzyme kinetics studies of spinach CA which have provided some answers to these questions. The results of our investigation reveal that while the active site of spinach CA is structurally very different from that of animal CA, the observed enzyme kinetics are consistent with a mechanism of action common to all known CAs, including the nature of the rate-determining step in catalysis.

EXPERIMENTAL PROCEDURES

Enzyme. Spinach carbonic anhydrase was purified using a modification of the method of Kandel et al. (1978). All purification steps were carried out at 4 °C. Approximately 4.5 kg of fresh spinach leaves were washed, destemmed, and cut into small pieces. The leaves were then pureed in small batches for 5 min in a blender using 20 mM sodium phosphate buffer (pH 6.8) containing 0.1 M NaCl and 1 mM EDTA. The homogenate (about 5 L) was filtered through two layers of cheesecloth, brought to 170 g/L $(NH_4)_2SO_4$, and stirred for 30 min. This solution was centrifuged at 5000*g* for 50 min, and the pellet was discarded. The supernatant was brought to a total of 290 g/L $(NH_4)_2SO_4$, stirred for 30 min, and again centrifuged at 5000*g* for 50 min. The pellet was resuspended in 100 mL of the phosphate buffer and exhaustively dialyzed against the same.

The dialyzed, crude extract was then applied to a 5 × 60 cm DEAE Sephacel column previously equilibrated with phosphate buffer, and eluted at 1 mL/min with the same. Active fractions, as determined by a modified Wilbur-Anderson assay (Rickli et al., 1946) were pooled and concentrated by ultrafiltration to 20 mL and applied to a 2.5 × 100 cm Bio-Gel A-1.5m column. The gel exclusion column was eluted with phosphate buffer at 0.5 mL/min, and active fractions were pooled and concentrated by ultrafiltration to 20 mL. In the final purification step, this sample was applied to a 5 × 50 cm DEAE Sephacel column equilibrated with 20 mM sodium phosphate buffer (pH 6.8) containing 0.1 M NaCl and 1 mM EDTA. The column was then eluted at 1 mL/min with the same buffer containing 0.15 M NaCl. The first, major peak of active fractions was pooled and concentrated to 15 mL by ultrafiltration. This preparation, typically about 500 mg, is colorless, and homogeneous by SDS–PAGE. It contains 1 mol of zinc per subunit (28 kDa) according to atomic absorption measurements. Protein concentrations were determined using the microbiuret method (Goa, 1953) or by the dye-binding method described by Bradford (1976). Spinach carbonic anhydrase solutions do not tolerate freezing/thawing or lyophilization but can be stored for many months at 4 °C without significant loss of activity. Upon prolonged storage at 4 °C, spinach carbonic anhydrase preparations darken significantly, and the last purification step must be repeated to remove colored contaminants.

Kinetics Methods. Saturated solutions of CO_2 were prepared by bubbling CO_2 gas into water in a vessel maintained at 25 ± 0.1 °C, and dilutions prepared in the absence of air by coupling two gas-tight syringes as described by Khalifah (1977). CO_2 concentrations were calculated based on a 33.8 mM (H_2O) or 38.1 mM (D_2O) saturated solution at 25 °C (Pocker & Bjorquist, 1977).

All steady-state kinetic measurements were made at 25 °C using a Hi-Tech SF-42 stopped-flow spectrophotometer interfaced with a Zenith Z-159 microcomputer and DAS-16 rapid data acquisition system. Reaction rates were measured using the changing-pH indicator method described previously (Khalifah, 1971; Ghannam et al., 1986; Rowlett et al., 1991).

In order to determine the solvent deuterium isotope effect on kinetic constants, we prepared identical buffer solutions in H_2O and D_2O and adjusted the solution pH until the pH meter readings were identical. This method is appropriate because the correction of a pH meter reading for pD [pD = (meter reading) + 0.4; Glasoe & Long, 1960)] is approximately compensated by the change in acid dissociation constant in D_2O for weak acids whose pK_a values lie between 3 and 10 [$pK_D - pK_H = 0.5 \pm 0.1$; Bell, 1959). Thus, by using the uncorrected pH meter reading, the relative ioniza-

tion states of relevant acidic groups on the enzyme and substrates will be comparable in both H_2O and D_2O (Venkatasubban & Silverman, 1980).

Analysis of Kinetic Data. The reaction velocity, v, was obtained from the initial slope of the progress curve according to eq 5, where Q is a buffer-dependent factor relating changes in absorbance to changes in $[H^+]$, and dA/dt is the initial slope of the progress curve:

$$v = \frac{d[H^+]}{dt} = Q\frac{dA}{dt} \quad (5)$$

All reaction velocities were corrected for the uncatalyzed reaction, which typically comprised less than 5% of the overall reaction rate. Kinetic parameters k_{cat} and K_m were determined by nonlinear least-squares regression analysis similar to that described by Cleland (1967) and were calculated on a per subunit basis using a subunit molecular mass of 28 kDa.

^{13}C-NMR Exchange. All ^{13}C-NMR line broadening experiments were carried out at 25 °C using a Bruker AC-250 FT-NMR operating at 62.9 MHz. Solutions of $NaH^{13}CO_3$ in 10% D_2O were prepared according to Simonsson et al. (1979). Bicarbonate ion ^{13}C line widths were measured in 5 mm NMR tubes with a dual ^{1}H/^{13}C probe, using a sweep width of 8064 Hz and a pulse length of 10 μs. NMR tubes were filled completely and sealed tightly with parafilm to prevent loss of CO_2 to the headspace or the atmosphere. Depending on the concentration of $H^{13}CO_3^-$ in the solution, 256−8192 pulses were necessary to obtain a satisfactory signal to noise ratio. Peak widths were determined by using a Lorentzian curve fit routine provided by Bruker. One hertz of artificial line broadening was added to all spectra in order to improve the signal to noise ratio.

EXAFS. EXAFS data were collected at the National Synchrotron Light Source on beamline X-9A. Spinach carbonic anhydrase samples, 65 mg/mL, were prepared in 20 mM sodium phosphate−1 mM EDTA buffer, pH 6.8. Human carbonic anhydrase I was prepared as described previously (Khalifah et al., 1977), and dissolved in distilled water to yield a solution of 24 mg/mL. All carbonic anhydrase solutions were titrated with 0.1 M NaOH to a pH of 9.0 ± 0.3 as measured by pH strips (ColorpHast, pH 6.5−10.0 range). Approximately 250 μL each of these samples were frozen in a lucite sample holder over liquid nitrogen. Frozen samples and holders were stored in liquid nitrogen until use. EXAFS spectra were collected at a temperature of 180 K.

The methods for collecting zinc EXAFS data and the model compounds used have been described previously (Summers et al., 1992; Chance et al., 1992) and are briefly summarized here. Silicon [111] crystals were used in the monochromator, and harmonics rejected using a mirror. The X-ray fluorescence data from the central zinc ion was collected using a 13-element energy resolving germanium detector, run at internal count rates of 40 000 counts per second without dead time corrections. Six scans for each enzyme sample were collected in 3 eV steps above the zinc edge with 4 s per point signal averaging from 30−450 eV above the edge and 6 s per point from there to the end of the scan. Model compound data was collected with an integrating detector as described in Chance et al. (1992). The data were manipulated to remove the contribution from the absorption edge, yielding "background corrected" spectra. These data were Fourier transformed to convert the background corrected spectra to a radial distribution function. The FT data are quite instructive, because they show the central metal environment directly. However, this Fourier transform data only shows the *relative* radial distances between Zn and scattering centers.

We measured the metal−ligand distances and Debye−Waller factors of scatterers by Fourier filtering, back-transforming, and nonlinear least-squares fitting of the CA data to model compounds (Lee et al., 1981; Lytle et al., 1989; Chance et al., 1986). The observed truncation artifacts were minimized by matching the window function of the model compounds and the unknowns. Thus, the model data were reduced, transformed, and back-transformed in a fashion identical to the unknown data, so that artifacts of the manipulations cancel out. We settled on k-space windows of 1.5−12 Å^{-1} for the forward Fourier transform and r-space windows of 1.0−2.6 Å for the Fourier filter window. With these windows the data were not extrapolated and sufficient degrees of freedom were available in a two-atom type fit (Lee et al., 1981; Lytle et al., 1989; Chance et al., 1986), because the data range for fitting is 4−11.5 Å^{-1}. The distance errors were estimated by a number of methods described previously (Lytle et al., 1989; Chance et al., 1986).

Data analysis with fixed coordination numbers was carried out as described previously using the University of Washington EXAFS package on a VAX computer (Chance et al., 1992). This analysis was checked against fits analyzed using the Bell labs EXAFS package run on a personal computer (Scheuring & Chance, 1994). We compared several fits with different nitrogen:sulfur (N:S) coordination numbers held fixed in the fitting procedure. The different contributions to the data can be resolved by applying fixed coordination numbers in the fitting procedure and searching for possible minima in parameter space (Summers et al., 1992; Chance et al., 1992; Lee et al., 1981; Lytle et al., 1989; Chance et al., 1986). Various parameters of coordination number were chosen to identify possible candidates for the metal−nitrogen and metal−sulfur distance solutions. For example, a 2:2 N:S fit used the zinc sulfide model compound to supply a contribution of two sulfur ligands, and zinc−tetraphenylporphyrin to supply a contribution of two nitrogen ligands. Using the EXAFS equation, this basis set was fit to the unknown data and the metal−ligand distances, Debye−Waller factors, and edge energies for the unknown were recorded along with the sum-of-residuals-squared (χ^2).

RESULTS

pH Dependence. Progress curves for the spinach CA-catalyzed hydration of CO_2 were found to be normal, and consistent with Michealis−Menten kinetics over the pH range of 6.5−9.5. The value of k_{cat} was found to be pH dependent, with an apparent pK_a of approximately 8.5 in the absence of sulfate ion (Figure 1). We found that sulfate ion, often used in CA kinetics studies to maintain constant ionic strength, was a significant inhibitor of spinach CA at all pH values. This inhibition is clearly shown in Figure 1. The pH dependence of spinach CA is similar in form to that of bovine CA III (Rowlett et al., 1991), and can be modeled by eq 6:

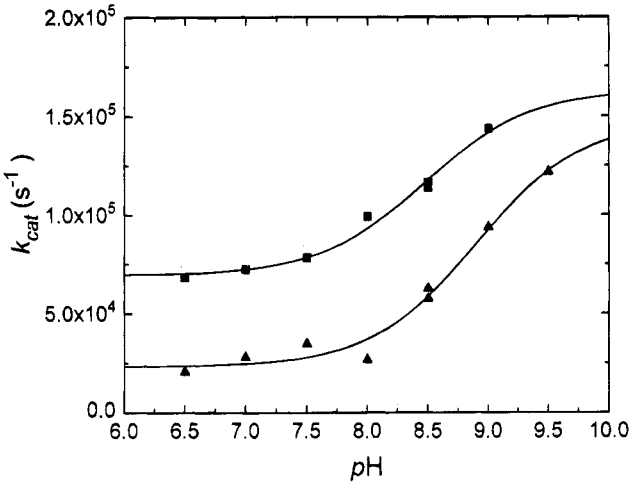

FIGURE 1: pH Dependence of k_{cat} for the CO_2 hydration reaction catalyzed by spinach CA. Reaction conditions were 40 mM buffer (MES, MOPS, HEPES, or bicine), 50–200 μM indicator dye (chlorophenol red, *p*-nitrophenol, phenol red, or *m*-cresol purple), 100–500 nM enzyme, 25 °C. Least squares analysis for data collected in the absence of Na_2SO_4 (■) gives $k_{cat}^{max} = (1.63 \pm 0.01) \times 10^5\ s^{-1}$, $k_{cat}^{min} = (6.95 \pm 0.28) \times 10^4\ s^{-1}$, $pK_a = 8.46 \pm 0.13$. Least squares analysis for data collected in the presence of 100 mM Na_2SO_4 (▲) gives $k_{cat}^{max} = (1.47 \pm 0.12) \times 10^5\ s^{-1}$, $k_{cat}^{min} = (2.33 \pm 0.37) \times 10^4\ s^{-1}$, $pK_a = 8.90 \pm 0.13$.

$$k_{cat}^{obs} = k_{cat}^{min} + \frac{k_{cat}^{max} - k_{cat}^{min}}{1 + \frac{[H^+]}{K_a}} \quad (6)$$

In eq 6, k_{cat}^{obs} is the observed value of k_{cat} at any given pH value, k_{cat}^{min} is the minimum, limiting value at low pH, k_{cat}^{max} is the maximum limiting value at high pH, and K_a is the apparent acid dissociation constant controlling the transition. Sulfate ion shifts the apparent pK_a value upward by approximately 0.4 pH units.

Sulfate Inhibition. The mode of sulfate ion inhibition of CO_2 hydration catalyzed by spinach CA is pH dependent. At low pH, a noncompetitive inhibition pattern is observed [reaction conditions: pH 6.5, 40 mM MES, 60 μM chlorophenol red, 1 mM EDTA, 180 nM enzyme, 25 °C; least-squares fit to a noncompetitive inhibition model gives $k_{cat} = (6.8 \pm 0.4) \times 10^4\ s^{-1}$, $K_m = 7.9 \pm 0.9$ mM, $K_i = 80 \pm 7$ mM], while at high pH, the inhibition pattern is clearly uncompetitive [reaction conditions: 40 mM bicine, 25 μM *m*-cresol purple, 1 mM EDTA, 180 nM enzyme, 25 °C; least-squares fit to a uncompetitive inhibition model gives $k_{cat} = (1.15 \pm 0.04) \times 10^5\ s^{-1}$, $K_m = 5.5 \pm 0.4$ mM, $K_i = 220 \pm 15$ mM]. At intermediate pH values, there is a smooth transition between the two modes of inhibition.

Inhibition by Small Molecules and Ions. We found that not only sulfate, but many other common cations and anions inhibit spinach carbonic anhydrase, some quite strongly. Alkylsulfonamides were poor inhibitors of spinach CA. A summary of these findings is listed in Table 1.

Measurement of the Rate of CO_2–HCO_3^- Exchange. Spinach CA catalyzes the rate of CO_2-HCO_3^- exchange as measured by ^{13}C-NMR line-broadening (Figure 2). For all data points in Figure 2, $\Delta\omega\cdot\tau \gg 1$ (the actual values vary from 300 to 1500), verifying that slow exchange conditions prevail. Under these conditions, the data of Figure 2 can be fit to eq 7 (Koenig et al., 1974).

Table 1: Some Inhibitors of Spinach CA[a]

inhibitor	K_i (mM)
ethylsulfonamide	52
SO_4^{2-}	43
Cl^-	33
n-hexylsulfonamide	16
methylsulfonamide	3.3
Co^{2+}	1.7
Zn^{2+}	0.27
NO_3^-	0.20
SCN^-	0.075
N_3^-	0.0077
Hg^{2+}	<0.001
Cu^{2+}	<0.001

[a] The following conditions were used: pH 7.0, 25 mM MOPS, 50 μM *p*-nitrophenol, and 200 nM enzyme, 25 °C; cations were supplied as the sulfate salt; anions were supplied as the sodium salt.

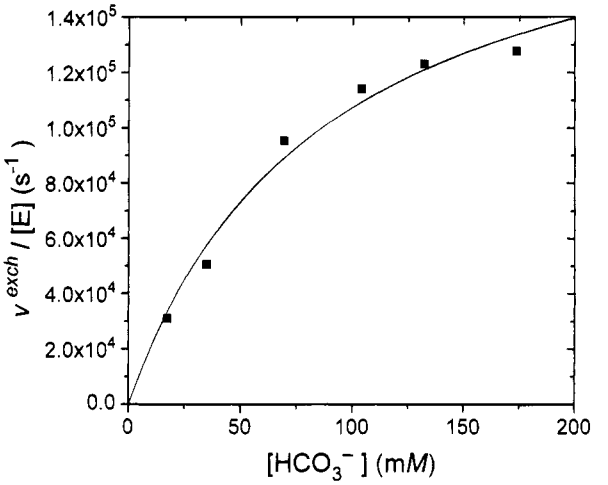

FIGURE 2: Rate of $CO_2 \rightleftharpoons HCO_3^-$ exchange reaction catalyzed by spinach CA. Reaction conditions were pH 7.0, 67 mM Na_2SO_4; 25 °C; $[HCO_3^-]$/[enzyme] ratio was maintained at 2800. Solutions contained 10% D_2O for signal locking purposes. Least squares analysis gives $k_{cat}^{exch} = (1.91 \pm 0.17) \times 10^5\ s^{-1}$, $K_{eff} = 75 \pm 16$ mM.

$$\frac{v^{exch}}{[E]} = \frac{k_{cat}^{exch}[HCO_3^-]}{K_{eff} + [HCO_3^-]} \quad (7)$$

In eq 7, v^{exch} is the catalyzed exchange rate, k_{cat}^{exch} is the maximal rate constant for exchange, and K_{eff} is the apparent Michaelis constant for the exchange reaction.

We found it necessary to include salt in the reaction mixture in order to prevent the enzyme from losing activity over the course of the NMR experiment. We chose to include Na_2SO_4, rather than NaCl in the reaction mixture for this purpose, because Na_2SO_4 is less inhibitory than NaCl. Under these conditions, we measured a maximal exchange rate of $(1.91 \pm 0.17) \times 10^5\ s^{-1}$ at 25 °C. At the same Na_2SO_4 concentration and pH, we also measured the maximal rates of CO_2 hydration and HCO_3^- dehydration by stopped-flow spectrophotometry. We determined a maximal rate constant for CO_2 hydration, $k_{cat}^{CO_2} = (3.40 \pm 0.12) \times 10^4\ s^{-1}$ (reaction conditions: pH 7.0, 67 mM Na_2SO_4, 25 mM MOPS, 50 μM *p*-nitrophenol, 180 nM enzyme, 25 °C), and a maximal rate constant for HCO_3^- dehydration, $k_{cat}^{HCO_3^-} = (5.20 \pm 0.14) \times 10^4\ s^{-1}$ (reaction conditions: pH 7.0, 67 mM Na_2SO_4, 100 mM HEPES, 25 μM phenol red, 1.5 μM enzyme, 25 °C).

Table 2: Solvent Deuterium Isotope Effect on the CO_2 Hydration Reaction Catalyzed by Spinach CA[a]

pH	$\frac{k_{cat}^{H}}{k_{cat}^{D}}$	$\frac{(k_{cat}/K_m)^{H}}{(k_{cat}/K_m)^{D}}$
6.0	1.70 ± 0.24	1.70 ± 0.50
7.0	1.90 ± 0.13	0.90 ± 0.22
9.0	2.09 ± 0.19	1.22 ± 0.37

[a] Reaction conditions were 40 mM buffer (MES, MOPS, and bicine at pH 6.0, 7.0, and 9.0, respectively), 50−200 μM indicator dye (chlorophenol red, *p*-nitrophenol, and *m*-cresol purple, respectively), and 100−500 mM enzyme, 25 °C. The pH values listed are uncorrected meter readings (see Experimental Procedures).

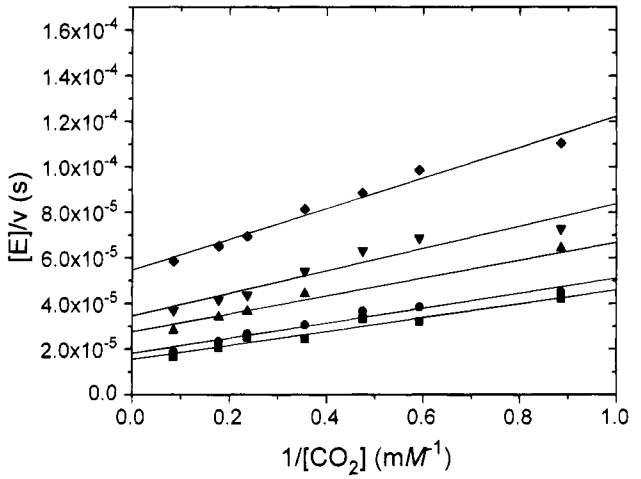

FIGURE 3: Lineweaver-Burk plot of the buffer dependence of the rate of spinach CA-catalyzed hydration of CO_2. Reaction conditions were pH 8.0, bicine buffer, 200 nM enzyme, 25 °C. Buffer concentrations are 20 mM (■), 10 mM (●), 5.0 mM (▲), 2.0 mM (▼), and 1.0 mM (♦).

Solvent Deuterium Isotope Effects. We have also measured the solvent deuterium isotope effect on k_{cat} and k_{cat}/K_m for the CO_2 hydration reaction in the absence of sulfate at pH values from 6 to 9. The results are summarized in Table 2. The solvent deuterium isotope effect on k_{cat} is relatively constant over the entire pH range of 6.0 to 9.0. For k_{cat}/K_m, the solvent deuterium effect is small over the entire pH range, and perhaps close to unity at pH 7.0 and 9.0.

Buffer Dependence of Catalysis. We found that the rate of the spinach CA-catalyzed hydration of CO_2 was strongly dependent on the concentration of buffer in the reaction medium. Buffer species behave kinetically as if they were a second substrate, yielding kinetic patterns suggestive of a ping-pong type mechanism (Figure 3). A replot of the k_{cat} values derived from the intercepts of Figure 6 yield an effective K_m for buffer of 3.9 mM at pH 8.0 (Figure 4). This value is typical for the apparent K_m of zwitterionic buffers used in the pH range 6.5−9.5. Thus, at buffer concentrations of 25 mM or higher, spinach CA is essentially "saturated" with respect to buffer.

EXAFS. The background-corrected spectrum for spinach CA is shown in Figure 5. Fourier transforms (radial distribution curves) of background-corrected EXAFS spectra for both spinach CA and human CA I are superimposed in Figure 6. The Fourier transform data reveals striking differences in structure between spinach CA and human CA I, the latter previously examined by Yachnadra et al. (1983). First is the significantly longer average distances for the

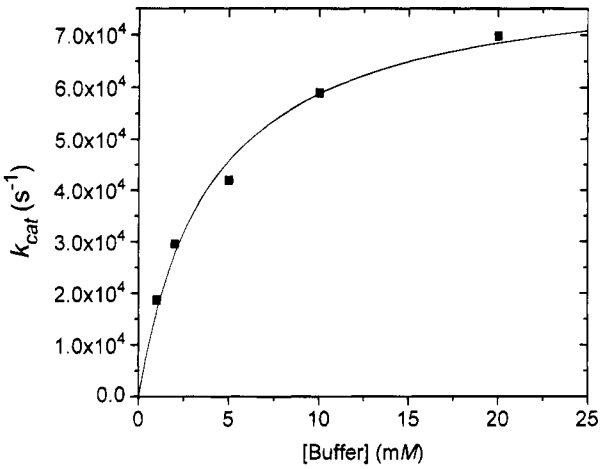

FIGURE 4: Replot of k_{cat} values obtained for the spinach CA-catalyzed hydration of CO_2 at various buffer concentrations. Reaction conditions were as in Figure 6. Least square analysis of the data yields $k_{cat} = (8.20 \pm 0.47) \times 10^4\ s^{-1}$; $K_m^{buffer} = 3.94 \pm 0.66$ mM.

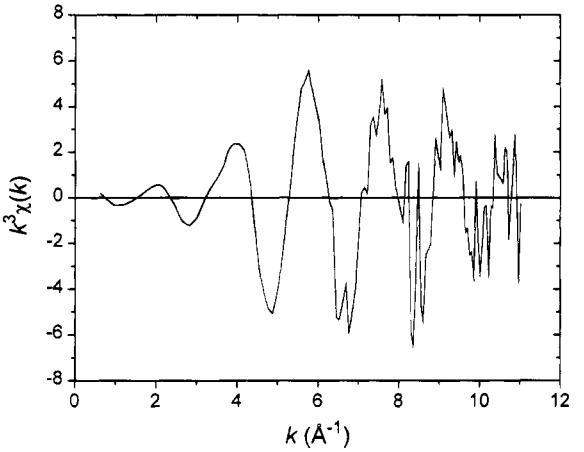

FIGURE 5: Background-subtracted, k^3-weighted EXAFS data for spinach CA.

spinach enzyme as evidenced by the shifts in the position of the first shell peak in the Fourier transform. Substantial differences in the higher shell data are also observed. Human CA I shows a significant back-scattering intensity at about 3.2 Å indicative of the α-carbons of the coordinated histidines. Different contributions are seen for spinach CA. The absence of back-scattering intensity cannot be taken as conclusive evidence of absence of atoms at that distance, due to potential disorder of the structure (Summers et al., 1992). However, this result is consistent with the sequence data indicating a low histidine content.

We analyzed human CA I data as a control in the analysis and compared the results to those reported previously (Yachandra et al., 1983). The results are shown in Table 3. The data is adequately fit with 4−5 ligands of nitrogen or oxygen character at an average distance of 2.01−2.02 Å. This is consistent with previous results. The higher shell data is also consistent with histidine coordination (data not shown). Table 3 also shows the result of forcing sulfur ligands onto the human CA I data. The program finds a "good fit" with respect to χ^2 but the Zn−S distances are chemically unreasonable (Vedani & Huhta, 1990), and therefore these solutions must be rejected (Scheuring & Chance, 1994). Thus, the absence of sulfur is required in the fitting of the human CA I data.

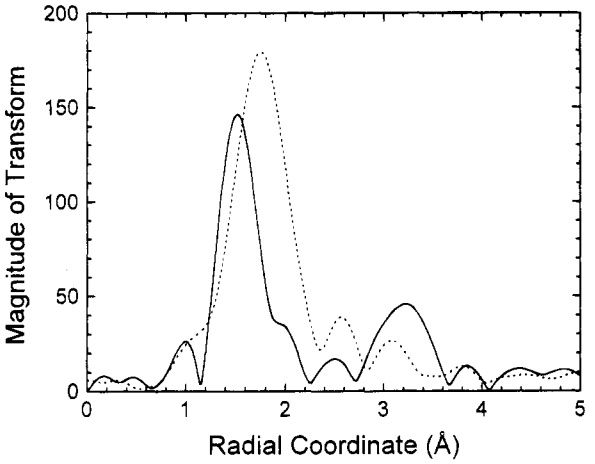

FIGURE 6: Fourier transformed EXAFS data for human CA I (—) and spinach CA (•••). Notice the increased first shell distance for the spinach enzyme and the greater distribution of distances indicated by the width of the first shell peak, compared to the human enzyme. The human enzyme also has obvious histidine α-carbon contributions in the higher shell. Any histidine contribution for the spinach enzyme is greatly reduced compared to that of the human enzyme.

Table 3: EXAFS Spectral Data for Human Carbonic Anhydrase I at pH 9.0

coordination no.	r (Å)[a]	χ^2	ΔE_0 (eV)[b]	$\Delta\sigma^2$ (Å^2)[c]
4	2.02	1.97	−4	0.00099
5	2.01	0.67	−2	0.0027
4.81 (not fixed)	2.02	0.64	−4	0.0025

coordination N:S	r_1, N[a] (Å)	r_2, S[d] (Å)	χ^2	ΔE_0, N[b] (eV)	ΔE_0, S[b] (eV)	$\Delta\sigma^2$, N[c] (Å^2)	$\Delta\sigma^2$, S[c] (Å)
3:1	1.98	**2.19**	0.37	6	5	0.0015	0.0051
4:1	1.99	**2.17**	0.35	5	4	0.0029	0.0068
5:1	2.00	**2.15**	0.35	0	4	0.0042	0.0062

[a] The average Zn−N bond distance. [b] The change in the edge energy relative to the reference compound. [c] The change in the Debeye−Waller factor, relative to the reference compound. [d] The average Zn−S bond distance. Entries in bold in this column are bond distances which are uncharacterized in the literature for a Zn−S bond length. These fits have therefore been ruled out at possible solutions.

In the absence of spectroscopic information that exactly defines the ligand coordination for spinach CA, a unique solution cannot be provided by EXAFS. Thus, we analyzed a series of fits based on known coordination of biological or bioinorganic zinc sites (Table 4). In each coordination model considered, we assumed a certain combination of coordinating ligands, and then found the combination of metal−ligand distances, Debeye−Waller disorder factors, and absorption edge shifts that gave the best fit to the data. The 2:2 N:S fit has the best χ^2 with average Zn−N distances of 1.99 Å and average Zn−S distances of 2.31 Å. The Zn−ligand distances observed are reasonable based on surveys of crystal structure data (Vedani & Huhta, 1990).

Individual Zn−S distances cannot be distinguished as the resolution of the data, or the ability to distinguish distances separated by less than 0.1 Å, is limited by the data range (Lee et al., 1981; Lytle et al., 1989). However, Zn−S and Zn−N distances can be easily resolved from one another. Also, N and O are generally not distinguishable from each other. Therefore, an implied Zn−N distance (for example to histidine) would not be distinguishable from a Zn−O distance to an oxygen-bearing ligand.

Table 4: EXAFS Spectral Data for Spinach Carbonic Anhydrase at pH 9.0

coordination N:S	r_1, N[a] (Å)	r_2, S[b] (Å)	χ^2 [c]	ΔE_0, N[d] (eV)	ΔE_0, S[d] (eV)	$\Delta\sigma^2$, N[e] (Å^2)	$\Delta\sigma^2$, S[e] (Å^2)
1:3	2.03	2.31	**5.24**	5	4	−0.002	0.002
2:2	1.99	2.31	0.58	6	5	−0.001	−0.002
3:1	2.02	2.32	2.96	2	5	−0.0024	−0.006
1:4	2.08	2.32	**8.26**	5	2	−0.0096	0.008
2:3	2.04	2.30	**5.51**	5	4	0.0072	0.0021
3:2	2.03	2.31	1.35	0	4	0.0047	−0.001
4:1	2.05	2.32	1.28	−4	5	0.0016	−0.0055
1:5	2.09	2.34	**11.66**	5	0	**−0.011**	**0.012**
3:3	2.06	2.31	**5.36**	5	2	**0.012**	0.0022
4:2	2.01	2.31	1.24	5	2	0.009	−0.001
5:1	2.06	2.31	0.68	−5	4	0.0050	−0.0050

[a] The average Zn−N bond distance. [b] The average Zn−S bond distance. [c] Entries in bold in this column have unacceptably high χ^2 values. These fits have therefore been ruled out at possible solutions. [d] The change in the edge energy relative to the reference compound. [e] The change in the Debeye−Waller factor, relative to the reference compound. Entries in bold in this column have unacceptably high Debeye−Waller factors. These fits have therefore been ruled out at possible solutions.

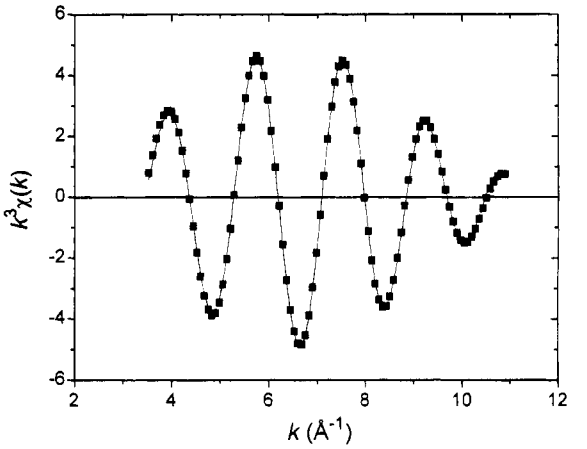

FIGURE 7: Fourier filtered first shell EXAFS data for spinach CA (■) compared to a simulation using a three nitrogen/one sulfur combination (—). A number of other simulations are also acceptable as shown in Table 4.

The 2:2 N:S fit is only one of a family of fits that may be considered possible solutions for the Zn-coordination sphere of spinach CA based *solely* on the Fourier filtered first shell EXAFS analysis. A 2:3 N:S fit is also reasonable with an acceptable χ^2 value, albeit 2.3 times higher than for a 2:2 N:S model. Figure 7 shows the simulation compared to the Fourier-filtered data, along with the residuals for the 3:1 N:S fit. A number of other fits are poor; for example, models with no nitrogen or sulfur contributions (0:n N:S or n:0 N:S, not shown) have extremely high χ^2 values. Also, a number of other fits have unreasonable χ^2 or Debye−Waller values (Summers et al., 1992; Chance et al., 1986, 1992; Lee et al., 1981; Lytle et al., 1989). These are shown in bold in Table 4. Figure 8 presents a graphic illustrating the range of reasonable solutions that we observe. These include possible Zn^{2+} environments with 4−6 ligands incorporating 1−2 sulfur ligands and 3−5 nitrogen or oxygen ligands. The overall data also tentatively suggest the absence of histidine ligands.

Previous investigations of the copper protein stellacyanin illustrated the difficulties in establishing the individual sulfur and nitrogen coordination numbers in cases where both are

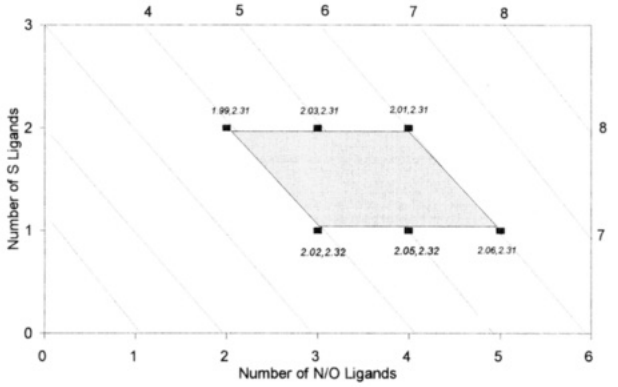

FIGURE 8: Schematic representation of acceptable Zn-coordination environments for spinach CA, based on EXAFS data (shaded region). Diagonal lines represent total coordination number. The pairs of numbers associated with individual data points on the plot represent average Zn−N and Zn−S bond distances, respectively.

present and the total coordination number is four or five (Peisach et al., 1982). This is due to the cross correlation of parameters in the fit, especially the coordination number and the Debye−Waller factors. Notice, in comparing the 1:3 N:S and 2:3 N:S fits for Tables 3 and 4, that the Debye−Waller factors opposite the fixed nitrogen contributions become more positive for the 2:3 N:S fit. The relationship of Debye−Waller factors and amplitudes for the EXAFS equation is such that a more positive Debye−Waller factor tends to reduce the amplitude, while increasing the coordination number has the opposite effect. Therefore, a range of solutions with comparable χ^2 values and Debye−Waller factors shifted less than 0.01 Å^2 from the models is unavoidable (Peisach et al., 1982).

DISCUSSION

All of the kinetics data we have reported here suggests that spinach CA has mechanism of action similar to that of the more well-known animal CA isoenzymes, namely the zinc-hydroxide mechanism described by eqs 2−4. However, the known amino acid sequence of spinach CA and the EXAFS data we have obtained, suggest that the active site structure of the plant enzyme is strikingly different from animal CA isoenzymes.

Efficiency of Catalysis. Spinach CA is of the same order of efficiency as animal CA isoenzymes. The maximal k_{cat} value for spinach CA at high pH is approximately 2×10^5 s^{-1} per subunit, compared to 1×10^6 s^{-1} for human CA II, and 2×10^5 s^{-1} for human CA I (Khalifah, 1971). Our limiting value for k_{cat} is slightly higher than the value of 8.8×10^4 s^{-1} reported by Pocker and Ng (1973) for the spinach enzyme at pH 9.0, and smaller than the values of 4×10^5 s^{-1} reported by Johansson and Forsman (1993) for the pea enzyme. We note, however, that Pocker and Ng (1974) included both chloride (typically 75 mM) and sulfate ion (up to 50 mM) in their reaction mixtures, both of which are inhibitors of spinach CA. The inhibition of spinach CA by these anions is sufficient to account for the discrepancy in limiting k_{cat} values for the spinach enzyme between our findings and those of Pocker and Ng (1974).

The pH profile k_{cat} for the spinach CA-catalyzed hydration of CO_2 increases with pH, suggesting the basic form of the enzyme is the active species. This is consistent with a zinc-hydroxide mechanism of action, where a Zn^{2+}-bound hydroxide ion, and not a Zn^{2+}-bound water molecule, is catalytically competent state in CO_2 hydration. While the pH profile can be modeled reasonably well by eq 6, yielding an effective pK_a of approximately 8.5, which is considerably higher than the apparent pK_a value of 7.0 observed for human CA II (Silverman & Lindskog, 1982), we hasten to add that the data is also consistent with a pH titration curve with multiple pK_a values. A similarly complex pH titration curve of k_{cat} was reported for pea CA.

Inhibition. Spinach CA is inhibited by a variety of small molecules and ions that are also inhibitors of animal CA isoenzymes. Both sulfate and chloride are reasonably strong inhibitors of spinach CA. By comparison, human CA II is insignificantly inhibited by sulfate at pH values above 6.5 (Simonsson & Lindskog, 1982), and the K_i for chloride inhibition of CA II is 190 mM at pH 6.8 (Behraven et al., 1990). Thus, sulfate inhibition of spinach CA appears to be intermediate between human CA II and bovine CA III, the latter of whichwhich is inhibited by sulfate with a K_i of 1.0 mM at pH 7.0 (Rowlett et al., 1991). In general, monovalent anions have K_i values for spinach CA that are 1−2 orders of magnitude smaller than for bovine CA II, and are roughly comparable to those for bovine CA III. To avoid artifactual contributions to our kinetic data, we used only zwitterionic buffers in this study, to avoid sulfate or small monovalent anion inhibition of the enzyme.

The kinetic patterns for the inhibition of spinach CA by sulfate are reminiscent of that for monovalent inhibition of human or bovine CA II (Pocker & Deits, 1982; Tibell et al., 1984): at low pH, kinetic patterns indicate noncompetitive inhibition; at high pH, kinetic patterns change to an uncompetitive inhibition pattern. It has been amply demonstrated that this kinetic pattern can be explained by the binding of anions to only the Zn^{2+}-water form of the enzyme, and that the shift in kinetic pattern coincides with the ionization of the Zn^{2+}-bound water molecule (Rowlett, 1984; Lindskog, 1984; Tibell et al., 1984). The observation of this inhibition pattern for sulfate ion suggests that it may be binding at the metal ion site, and that the pK_a for the putative Zn^{2+}-bound water may be in the pH range of 6.5 to 9.0.

It is also rather interesting that a number of metal cations strongly inhibit spinach CA. In particular, Cu^{2+} and Hg^{2+} are powerful inhibitors of spinach CA, and Zn^{2+} and Co^{2+} to a lesser extent. Both Cu^{2+} and Hg^{2+} are inhibitors of human CA II at the sub-micromolar level (Tu et al., 1981; Kararli & Silverman, 1984). X-ray crystallography has shown that these inhibitors act by binding to a histidine residue in the active site of CA II which is responsible for "shuttling" H^+ ions from Zn^{2+}-bound water to the bulk medium (Eriksson et al., 1986). While it is possible that Cu^{2+} and Hg^{2+} ions inhibit spinach CA by combining with one or more of the many cysteine residues in the protein, it may also be possible that a proton shuttle group is being inhibited. We note that Zn^{2+} inhibits both human CA II and spinach CA in a reversible fashion.[2] It is quite likely that Zn^{2+} inhibits human CA II by the same mechanism as Cu^{2+} or Hg^{2+} ion.

Finally, we note that the inhibition of spinach CA by *n*-alkylsulfonamides is approximately 3 orders of magnitude smaller than for human CA II (Rowlett et al., 1992). Similar

[2] R. S. Rowlett and Jill R. Royal, unpublished observations.

results have been reported by others for the inhibition of plant CA by a variety of arylsulfonamides (Pocker & Ng, 1974, Johansson & Forsman, 1993). It has been proposed that the active site of plant CA is too small to accommodate the bulky arylsulfonamide inhibitors that are so effective against animal CA isoenzymes (Pocker & Ng, 1974), but it appears that the less bulky alkylsulfonamides are no better, and perhaps worse, as inhibitors of spinach CA.

The Rate-Determining Step in Catalysis. Our ^{13}C-NMR data, taken in conjunction with steady-state kinetics measurements under the same experimental conditions, are entirely consistent with the protolysis of water (eq 4) being the rate-determining step in a zinc-hydroxide mechanism for spinach CA. If instead, the interconversion of CO_2 and HCO_3^- were rate-limiting in spinach CA catalysis, then one would expect sum of the lifetimes of the forward (CO_2 hydration) and reverse (HCO_3^- dehydration) reactions at steady state to be approximately equal to the $CO_2 \rightleftharpoons HCO_3^-$ exchange lifetime (Simonsson et al., 1979, 1982):

$$\tau_{hyd} + \tau_{dehyd} \approx \tau_{exch} \quad (8)$$

Since $\tau = (1/k_{cat})$, we can show that $\tau_{hyd} = 29\ \mu s$, $\tau_{dehyd} = 19\ \mu s$, and $\tau_{exch} = 5.2\ \mu s$ at pH 7.0. Thus, we find that $\tau_{hyd} + \tau_{dehyd} \gg \tau_{exch}$ ($48\ \mu s \gg 5.2\ \mu s$), so that some other step besides those involving the interconversion of CO_2 and HCO_3^- must be rate-limiting in the overall reaction. Thus, we are left to assume the protolysis of water (eq 4) must be the rate-determining step in overall catalysis.

This conclusion is bolstered by the solvent deuterium isotope effect on k_{cat} for the CO_2 hydration reaction catalyzed by spinach CA. We find a relatively constant isotope effect of 2.0 on k_{cat} over the pH range 6.0 to 9.0. This isotope effect is somewhat smaller than the value of 3.8 observed for human CA II (Steiner et al., 1975), but similar to that observed for bovine CA III (Rowlett et al., 1991). A deuterium isotope effect is expected if there is a rate-determining H^+ transfer in the catalytic mechanism. We find that there is virtually no solvent deuterium isotope effect on the k_{cat}/K_m ratio for the spinach CA-catalyzed hydration of CO_2. This result is expected in the zinc-hydroxide mechanism, where the isotope effect on k_{cat}/K_m is governed only by steps up to and including the release of HCO_3^- (eqs 2 and 3), none of which include an explicit H^+ transfer.

Buffer Dependence of Catalysis. The kinetic patterns obtained for the buffer activation of spinach CA (Figures 5 and 6) are consistent with external buffers acting as a second substrate for the enzyme. Similar kinetic behavior is observed for the buffer activation of human CA II (Jonsson et al., 1976; Rowlett & Silverman, 1982) and for pea CA (Johansson & Forsman, 1993). Such ping-pong like kinetic patterns are indicative of buffer interacting with the enzyme separate from and subsequent to the conversion and release of HCO_3^- (eqs 2−3). The observed kinetic data is expected if buffer species, and not bulk water are the ultimate H^+ acceptor in eq 4. Indeed, the maximal k_{cat} value for a carbonic anhydrase following the zinc-hydroxide mechanism (eqs 2−4) would be on the order of 1000 s^{-1} if water is the ultimate H^+ acceptor (Rowlett & Silverman, 1982; Rowlett et al., 1991). Buffer participation in the protolysis of the Zn^{2+}-bound water is not only expected, but required to account for the maximal k_{cat} value of 2×10^5 s^{-1} for spinach CA at high pH.

We did not observe any anomalous kinetic behavior of spinach CA with the zwitterionic buffers used in this study. Pocker and Ng (1973) reported that phosphate activated spinach CA, while other buffers (mostly imidazole derivatives) were inhibitors of spinach CA. We believe that the inhibition of spinach CA by imidazole type buffers can be explained by the presence of chloride and/or sulfate counterions in these buffer systems; phosphate buffers should not normally contain any inhibitory counteranions, and should therefore activate spinach CA. Therefore, we do not believe that our buffer activation data is inconsistent with previous studies of spinach CA.

It has been shown that the k_{cat}/K_m^{buffer} ratio, where K_m^{buffer} is the effective K_m for buffer as a second substrate, provides an upper limit for the rate of H^+ transfer from CA to buffers in the bulk solution (Jonsson et al., 1976; Rowlett & Silverman, 1982). In human CA II, the k_{cat}/K_m^{buffer} ratio is approximately 1×10^9 M^{-1} s^{-1}, near the diffusion-controlled limit. Thus, for CA II, this places the source of the pH-independent solvent deuterium isotope effect on k_{cat} in a putative *intramolecular* proton transfer between Zn^{2+}-bound water and a nearby basic amino acid residue, now unambiguously identified as His-64 (Tu et al., 1989). In spinach CA, the k_{cat}/K_m^{buffer} ratio at pH 8.0 is only 2.1×10^7 M^{-1} s^{-1}, far short of diffusion control. Thus, it is impossible to conclude at this time if there is or is not an intramolecular H^+ transfer step in the mechanism of spinach CA.

Structure of the Active Site. The EXAFS data clearly indicates the coordination sphere of Zn^{2+} in spinach CA is quite different from animal CA isoenzymes. While the most likely coordination number for the Zn^{2+} in spinach CA is four, there must be at least one sulfur ligand, the remainder nitrogen or oxygen. It is presumed that at least one of the Zn^{2+} ligands is a water molecule which is essential for catalytic activity.

Vallee and Auld (1990) surveyed a dozen zinc-metalloenzymes whose amino acid sequence and X-ray crystallographic structure is known. This survey identified a number of recurrent Zn^{2+}-coordination schemes which allow us to make an educated guess about which amino acid residues in spinach CA may be involved in Zn^{2+}-binding. For all such known zinc metalloenzymes, the Zn^{2+}-ligating amino acids are either Cys, His, Asp, or Glu, and the Zn^{2+} coordination sphere is tetradentate. Histidine is the most common Zn^{2+} ligand. For zinc metalloenzymes with a Zn^{2+}-bound water molecule, the remaining three ligating amino acids are typically arranged in the sequence so that two of the ligands are close together in the amino acid sequence, separated by only 1−3 amino acid residues; the remaining ligand typically appears toward the carboxy terminus of the protein, separated from the first pair of ligands by 20−100 amino acids. In the four higher plant CAs whose sequences are now known, there are 18 conserved residues that could possibly ligate Zn^{2+}: 3 Asp, 7 Glu, 3 His, and 5 Cys. Examination these sequences reveals three likely loci for Zn^{2+} coordination. One site is defined by Cys-58 and His-61.[3] A second possible site is defined by His 112 and Cys 115. A third likely Zn^{2+} coordination site is defined by Cys-

[3] The amino acid numbering system is based on the N-terminal sequence analysis of spinach CA (Burnell et al., 1990), which is ELADGGTPSASYPVQRIKEG.

162 and Cys-165. Pending an X-ray crystallographic structure, these amino acid locations might be likely targets for site-specific mutagenesis experiments designed to locate the Zn^{2+}-binding site. Provart et al. (1993) have found that the pea CA mutants C52S, E96A, H112N, and C115S produce inactive protein. It is interesting to note that Cys-52, His-112, and Cys-115 would form a Zn^{2+}-ligating triad that is consistent with typical Zn^{2+} coordination patterns noted by Vallee and Auld (1990), and with our EXAFS data.

It is worthwhile to consider what effect the presence of one or more thiolate ligands would have on the chemistry of the Zn^{2+}-bound water molecule in spinach CA, compared to the all-nitrogen ligated animal CAs. Intutitively, one might expect that the presence of thiolate ligands would render Zn^{2+} a weaker Lewis acid, and thus raise the pK_a of the metal-bound water molecule. Such a conclusion would be in consonance with the observation that the pH profile of spinach CA is associated with a higher apparent pK_a than observed for animal CA isoenzymes. A detailed characterization of Zn^{2+} model compounds of CA has been limited to four- and five-coordinate species which contain all nitrogen ligands (Woolley, 1975; Kimura et al., 1990; Alsfasser et al., 1991). No analogous compounds containing sulfur ligands have been similarly characterized. However, site-specific mutagenesis of human CA II may offer some useful insight into the relationship between the acidity of Zn^{2+}-bound water and the nature of the ligating species. In a H94D mutant of human CA II, in which a ligating histidine has been changed to a negatively charged residue, the pK_a of the Zn^{2+}-bound water increases from 6.8 to $\geq$9.6 (Kiefer et al., 1993). Alexander et al. (1993) report constructing an even more relevant H94C mutant, but did not report a pK_a value for the Zn^{2+}-bound water molecule. Clearly, additional model studies and/or CA mutant characterization studies are needed.

Conclusions. The kinetics studies we report here for spinach CA are entirely consistent with a zinc-hydroxide mechanism of action which is well-established for animal CA isoenzymes. The functional similarity of spinach CA to animal CAs extends to its overall catalytic efficiency, a rate-determining H^+ transfer step in the catalytic mechanism, and to the participation of buffer as a second "substrate". However, it seems clear that the active site organization of spinach CA is quite different from that of animal CAs. It thus appears that nature solved the carbonic anhydrase catalysis problem twice: plant and animal CAs are convergently and nearly equally functionally evolved enzymes. A detailed structural comparison of these two CAs should be fertile ground for developing an understanding of carbonic anhydrase catalysis.

ACKNOWLEDGMENT

We thank Dr. Gregory Petsko for providing amino acid sequence homology analysis for plant carbonic anhydrases.

REFERENCES

Alexander, R. S., Kiefer, L. L., Fierke, C. A., & Christianson, D. W. (1993) *Biochemistry 32*, 1510−1518.

Aliev, D. A., Guliev, N. M., Mamedov, T. G., & Tsuprun, V. L. (1986a) *Biokhimiya 51*, 1785−1794.

Aliev, D. A., Tsuprun, V. L., Guliev, N. M., & Mamedov, T. G. (1986b) *Dokl. Akad. Nauk. SSSR 285*, 1472−1475.

Alsfasser, R., Trofimenko, S., Looney, A., Parkin, G., & Vahrenkamp, H. (1991) *Inorg. Chem. 30*, 4098−4100.

Behraven, G., Jonsson, B.-H., & Lindskog, S. (1990) *Eur. J. Biochem. 190*, 351−357.

Bell, R. P. (1959) *The Proton in Chemistry*, Chapter XI, Cornell University Press, Ithaca, NY.

Bradford, M. M. (1976) *Anal. Biochem. 72*, 248−254.

Brundell, J., Falkbring, S. O., & Nyman, P. O. (1972) *Biochim. Biophys. Acta 284*, 311.

Carter, M. J. (1972) *Biol. Rev. 47*, 465.

Chance, M. R., Powers, L., Kumar, C., & Chance, B. (1986) *Biochemistry 25*, 1259−1265.

Chance, M., Sagi, I., Wirt, M. D., Frisbie, S. M., Scheuring, E., Chen, E., Bess, J. W., Henderson, L. E., Arthur, L. O., South, T. L., Perez-Alvarado, G., & Summers, M. F. (1992) *Proc. Natl. Acad. Sci. U.S.A. 89*, 10041−10045.

Eriksson, A. E. (1988) Ph.D. Dissertation, *Structural Differences between High and Low Activity Forms of Carbonic Anhydrases*, Uppsala University, Uppsala, Sweden.

Eriksson, A. E., Jones, T. A., & Liljas, A. (1986) In *Zinc Enzymes* (Bertini, I., Luchinat, C., Maret, W., & Zeppezauer, M., Eds.) p 317, Birkhauser, Boston.

Eriksson, A. E., Jones, T. A., & Liljas, A. (1988) *Proteins: Struct. Funct. Genet. 4*, 274−282.

Glasoe, P. K., & Long, F. A. (1960) *J. Phys. Chem. 64*, 188.

Jonsson, B.-H., Steiner, H., & Lindskog, S. (1976) *FEBS Lett. 64*, 310−314.

Johansson, I.-M., & Forsman, C. (1993) *Eur. J. Biochem. 218*, 439−446.

Kannan, K. K., Notstrand, B., Fridborg, K., Lovgren, S., Ohlsson, A., & Petef, M. (1975) *Proc. Natl. Acad. Sci. U.S.A. 72*, 51.

Kararli, T., & Silverman, D. N. (1984) *J. Protein Chem. 3*, 357−367.

Khalifah, R. G. (1971) *J. Biol. Chem. 246*, 2561−2573.

Khalifah, R. G., Strader, D. J., & Gibson, S. M. (1977) *Biochemistry 16*, 2241−2247.

Kiefer, L. L., Ippolito, J. A., Fierke, C. A., & Christianson, D. W. (1993) *J. Am. Chem. Soc. 113*, 12581−12582.

Kimura, E., Shiota, T., Koike, T., Shiro, M., & Kodama, M. (1990) *J. Am. Chem. Soc. 112*, 5805−5811.

Koenig, S. H., Brown, R. D., London, R. E., Needham, T. E., & Matwiyoff, N. A. (1974) *Pure Appl. Chem. 40*, 103−113.

Lee, P., Citrin, P., Eisenberger, P., & Kincaid, B. (1981) *Rev. Mod. Phys. 53*, 769−806.

Liljas, A., Kannan, K. K., Bergsten, P. C., Waara, I., Fridborg, K., Strandberg, B., Carbon, U., Jarup, L., Lovgren, S., & Petef, M. (1972) *Nature New Biol. 235*, 131.

Lindskog, S. (1984) *J. Mol. Catal. 23*, 357−368.

Lytle, F., Sayers, D., & Stern, E. (1989) *Physica B (Amsterdam) 158*, 701−722.

Majeau, N., & Coleman, J. R. (1992) *Plant Physiol. 100*, 1077−1078.

Maren, T. H. (1967) *Physiol. Rev. 47*, 503.

Neish, A. C. (1939) *Biochem. J. 33*, 300−308.

Peisach, J., Blumberg, W. H., Powers, L., & Chance, B. (1982) *Biophys. J. 38*, 277−285.

Pocker, Y., & Ng, J. S. Y. (1973) *Biochemistry 12*, 5127−5134.

Pocker, Y., & Ng, J. S. Y. (1974) *Biochemistry 13*, 5116−5120.

Pocker, Y., & Miksch, R. R. (1978) *Biochemistry 17*, 1119−1125.

Pocker, Y., & Deits, T. L. (1982) *J. Am. Chem. Soc. 104*, 2424−2434.

Provart, N. J., Majeau, N., & Coleman, J. R. (1993) *Plant Mol. Biol. 22*, 937−943.

Raines, C. A., Horsnell, P. R., Holder, C., & Lloyd, J. C. (1992) *Plant Mol. Biol. 20*, 1143−1148.

Reed, M. L. (1979) *Plant Physiol. 63*, 216−217.

Reed, M. L., & Graham, D. (1971) *Nature New Biol. 231*, 81.
Reed, M. L., & Graham, D. (1977) *Aust. J. Plant Physiol. 4*, 87.
Reed, M. L., & Graham, D. (1980) *Prog. Phytochem. 7*, 47.
Rowlett, R. S. (1984) *J. Protein Chem. 3*, 369−93.
Rowlett, R. S., & Silverman, D. N. (1982) *J. Am. Chem. Soc. 104*, 6737−6741.
Rowlett, R. S., Gargiulo, N. J., Santoli, F. A., Jackson, J. M., & Corbett, A. C. (1991) *J. Biol. Chem. 266*, 933−941.
Rowlett, R. S., Carter, R. A., Tsen, W., Santoli, F. A., Shiraki, W. W., & Klysa, T. (1992) *Biochem. (Life Sci. Adv.) 11*, 5−11.
Scheuring, E. M., & Chance, M. R. (1994) *Biochemistry 33*, 6310−6315.
Silverman, D. N., & Vincent, S. H. (1983) *CRC Crit. Rev. Biochem. 14*, 207−255.
Silverman, D. N., & Lindskog, S. (1988) *Acc. Chem. Res. 21*, 30−36.
Simonsson, I., & Lindskog, S. (1982) *Eur. J. Biochem. 123*, 29−36.
Simonsson, I., Jonsson, B.-H., & Lindskog, S. (1979) *Eur. J. Biochem. 93*, 409−417.
Simonsson, I., Jonsson, B.-H., & Lindskog, S. (1982) *Eur. J. Biochem. 129*, 163−169.
Steiner, H., Jonsson, B.-H., & Lindskog, S. (1975) *Eur. J. Biochem. 59*, 253−259.
Summers, M. F., Henderson, L. E., Chance, M. R., Bess, J. W., South, T. L., Blake, P. R., Sagi, I., Perez-Alvarade, G., Sowder, R. C., Hare, D. R., & Arthur, L. O. (1992) *Protein Sci. 1*, 563−574.
Tashian, R. E. (1989) *Bioessays 10*, 186.
Tibell, L., Forsman, C., Simonsson, I., & Lindskog, S. (1984) *Biochim. Biophys. Acta 789*, 302−310.
Tobin, A. J. (1970) *J. Biol. Chem. 245*, 2656−2666.
Tu, C. K., Wynns, G. C., & Silverman, D. N. (1981) *J. Biol. Chem. 256*, 9466−9470.
Tu, C. K., Silverman, D. N., Forsman, C. F., Jonsson, B.-H., & Lindskog, S. (1989) *Biochemistry 28*, 7913−7918.
Vallee, B. L., & Auld, D. S. (1990) *Biochemistry 29*, 5647−5659.
Venkatasubban, K. S., & Silverman, D. N. (1980) *Biochemistry 19*, 4984−4989.
Vedani, A., & Huhta, D. W. (1990) *J. Am. Chem. Soc. 112*, 4759−4767.
Woolley, P. (1975) *Nature 258*, 677−682.
Yachandra, V., Powers, L., & Spiro, T. G. (1983) *J. Am. Chem. Soc. 105*, 6596−6604.